

CRISPR-mediated protein-tagging signal amplification systems for efficient transcriptional activation and repression in *Saccharomyces cerevisiae*

Haotian Zhai, Li Cui, Zhen Xiong, Qingsheng Qi^{ID} and Jin Hou^{ID*}

State Key Laboratory of Microbial Technology, Shandong University, Qingdao, 266237, P.R. China

Received January 08, 2022; Revised April 24, 2022; Editorial Decision May 13, 2022; Accepted May 17, 2022

ABSTRACT

Saccharomyces cerevisiae is an important model eukaryotic microorganism and widely applied in fundamental research and the production of various chemicals. Its ability to efficiently and precisely control the expression of multiple genes is valuable for metabolic engineering. The clustered regularly interspaced short palindromic repeats (CRISPR)-mediated regulation enables complex gene expression programming; however, the regulation efficiency is often limited by the efficiency of pertinent regulators. Here, we developed CRISPR-mediated protein-tagging signal amplification system for simultaneous multiplexed gene activation and repression in *S. cerevisiae*. By introducing protein scaffolds (SPY and SunTag systems) to recruit multiple copies of regulators to different nuclease-deficient CRISPR proteins and design optimization, our system amplified gene regulation efficiency significantly. The gene activation and repression efficiencies reached as high as 34.9-fold and 95%, respectively, being 3.8- and 8.6-fold higher than those observed on the direct fusion of regulators with nuclease-deficient CRISPR proteins, respectively. We then applied the orthogonal bifunctional CRISPR-mediated transcriptional regulation system to regulate the expression of genes associated with 3-hydroxypropanoic acid production to deduce that CRISPR-associated regulator recruiting systems represent a robust method for simultaneously regulating multiple genes and rewiring metabolic pathways.

INTRODUCTION

Saccharomyces cerevisiae is a prominent cell factory for industrial applications (1,2). Gene expression regulation in a precise, robust manner is essential for diverse cellular processes. In metabolic engineering, accurately regulating the

expression of key metabolic pathway-associated genes is pivotal. For gene regulation, the gene editing system involving clustered regularly interspaced short palindromic repeats (CRISPRs) has been adapted by targeting nuclease-deficient CRISPR proteins to the transcription regulation region (3). CRISPR activation (CRISPRa) or interference (CRISPRi) can be achieved by fusing nuclease-deficient CRISPR proteins, such as nuclease-deficient Cas9 (dCas9), with activation or repression domains, respectively. The easily programmable single guide RNA (gRNAs) endows this CRISPR-mediated system the ability to target almost to any region of the genome with high efficiency and specificity. When coupled with gRNAs libraries, CRISPR-mediated systems can prove to be a valuable tool for genome-wide studies of gene regulation.

Several CRISPRa/i systems have been developed to date. Direct fusion of the effector protein with activation or repression domains is a frequently used approach for CRISPR regulation. Various transcription repressors, such as myc-associated factor X-interacting protein 1 (Mxi1) and the Krüppel-associated box domain of Kox1 (4), have been reported to be fused with dCas9 for CRISPRi. Similarly, the fusion of activation proteins, such as virion protein 64 (VP64) and p65 can enhance gene expression when targeting dCas9 to the regions in close proximity to the promoter (4,5).

The fusion of only one transcription effector often cannot achieve efficient transcriptional regulation; thus, to increase the effectiveness of transcriptional regulation, hybrid transcription effectors with several activation or repression domains have been designed. The hybrid tripartite activator, VP64-p65-Rta (VPR) was designed to fuse with dCas9 and the RNA expression was shown to be 22- to 320-fold greater than dCas9-VP64 in mammalian cells (6). A study tested variants of several repressor domains in yeast, and a tripartite repression domain engineered with TUP1, MIG1 and UME6 also amplified the repression effect by 5-fold (7–10). However, the number of direct fusion proteins remains limited, which restricts the regulation efficiency. In general, transcription initiation occurs via a series of sequential steps involving the coordinated action of several

*To whom correspondence should be addressed. Tel: +86 532 5863 2401; Email: houjin@sdu.edu.cn

transcription factors (11). To mimic the natural process, recruiting more transcription effectors to the promoter region can potentially increase transcriptional activation or repression. For this purpose, the development of tools, such as RNA (12,13) or protein scaffolds (14,15), has been reported. For example, the protein scaffold SunTag was combined the dCas9 system to recruit multiple VP64 activator for the activation signal amplification. Such systems have been mainly developed in mammalian cells and also in a few other species (16,17). Despite the importance of *S. cerevisiae* as a key model organism and a microbial cell factory, a comprehensive protein scaffold-mediated CRISPR regulation systems have not been reported. In addition, only single direction of regulation was reported using protein scaffolds, detailed characterization of protein scaffold-mediated CRISPR system for simultaneous gene repression and activation, which is crucial for multiplexed gene regulation, particularly in *S. cerevisiae*, is much needed.

Herein, we constructed two protein scaffold-mediated signal amplification systems, namely SPY and SunTag, and combined them with different nuclease-deficient CRISPR proteins, dCas9 and dCpf1, respectively, to establish a simultaneous gene activation and repression system in *S. cerevisiae*. The SunTag system (14), consists of multiple copies of the 19 residues GCN4 peptide and a single-chain variable fragment (scFv) of the anti-GCN4 antibody as a tag. It has been combined with CRISPR for base editing and gene regulation as well as to induce methylation and demethylation in mammalian and plant cells (18–22). The peptide chains can recruit multiple copies of tagged proteins for signal amplification. In addition, we expressed SpyCatcher/SpyTag in *S. cerevisiae* and determined its capability to recruit effectors. SpyTag (13 residues peptide) and SpyCatcher (the 116 residues complementary domain) are constructed by splitting the Cnab2 domain from the fibronectin-binding protein FbaB from *Streptococcus pyogenes*, and they can spontaneously reconstitute to form a covalent isopeptide bond under mild physiological conditions when simply mixed (23,24). The SpyTag/SpyCatcher system has been widely used for protein assembly (25), but it has not been applied as yet for signal amplification in *S. cerevisiae*. Our CRISPR-mediated protein-tagging signal amplification systems system was systematically optimized by engineering transcription effectors and peptide arrays. In comparison with the direct fusion of dCas9 with transcription effectors, this refined system showed much better activation and repression efficiency. Moreover, we used this system to simultaneously regulate multiple gene targets in a metabolic pathway to improve 3-hydroxypropanoic acid (3-HP) production.

MATERIALS AND METHODS

Strains and cultivation conditions

Escherichia coli strains Trans5 α and Trans2-Blue (Beijing TransGene Biotech, CO., LTD, China), which was used for constructing and propagating plasmids, were grown in Luria–Bertani media (10 g/l NaCl, 10 g/l tryptone, and 5 g/l yeast extract) supplemented with 100 mg/l ampicillin at 37°C. *S. cerevisiae* CEN.PK2-1C was used as the initial

strain for CRISPR regulation system construction and 3-HP production. Yeast strains were cultivated in YPD media containing 1% yeast extract, 2% peptone, and 2% glucose, and recombinant strains were grown on synthetic complete (SC) dropout media comprising 0.5% ammonium sulfate, 0.17% yeast nitrogen base (BBI Life Science Corporation, China), complete supplement mixture (without uracil, histidine, or leucine) (Sunrise Science Products, United States), and 2% glucose. For selection, 250 mg/l hygromycin B (HygB, Beijing DingGuo Changsheng Biotechnology Co., Ltd, China) was used.

Plasmids and strain constructions

Features of nuclease-deficient CRISPR proteins were listed in Supplementary Table S1. All recombinant and gRNA or crRNA plasmids are listed in Supplementary Tables S2 and S3, respectively. Primers used for gene amplification and gRNA/crRNA construction were synthesized by GeneWiz (Tianjin, China). Recombinant plasmids were constructed by traditional restriction digestion/ligation or the Gibson assembly method, and gRNA/crRNA plasmids were constructed using the Golden Gate assembly approach (26). Phanta Max Super-Fidelity DNA Polymerase was purchased from Vazyme Biotech Co. Ltd. (Nanjing, China). Restriction enzymes, T4 ligase, and Gibson reagent kits were obtained from Thermo Scientific (Waltham, MA). Yeast strains were transformed using the LiAc method; recombinant strains are listed in Supplementary Table S4.

For reporter gene expression, the integration plasmid pRS304-LEU2-GFP, comprising the *LEU2* promoter, *eGFP* gene, and *PGK1* terminator, was constructed using the Gibson assembly method. To assess the repression and activation efficiency of CRISPR system to other promoters, the *LEU2* promoter was replaced to weak or inducible promoters *GAL7p*, *HED3p*, *CYC1p* and *RNR2p* and the strong promoters *HHF2p*, *PGK1p*, *ENO2p* and *ENO1p* from *Kluyveromyces lactis*, respectively. The plasmid strains were then linearized and integrated into the *TRP1* locus of CEN.PK2-1C.

dCas9 was obtained in PCR reaction using the plasmid pTPGI-dCas9 as a template (27). The transcriptional regulatory domains Med2 (full length), Med2t (156–258 fused with 380–431aa), MIG1(481–504aa), and TUP1(73–129aa) were amplified from the genome of CEN.PK2-1C. Codon-optimized *dCpf1*, *VPR*, and *Mxi1* were synthesized by GenScript (Nanjing, China). To construct pIYC04-dCas9-Med2 and pIYC04-dCpf1-MIG1, activator or repressor encoding gene was fused to dCas9 or dCpf1 by GSGSGSGS or GSSKLGGSGGS linker, respectively, and then assembled to yeast 2 μ plasmid pIYC04 under the control of the *PGK1* promoter via *BamHI/SalI* digestion and ligation. The *Med2* fragment of pIYC04-dCas9-Med2 and *MIG1* fragment of pIYC04-dCpf1-MIG1 was then replaced by *BamHI/SalI* digestion to construct dCas9 and dCpf1, respectively, with different transcriptional regulatory domains. To construct pIYC04-NLS-dCas9/dCpf1-2 \times NLS-GCN4tag (linker GSGSG was used) and pIYC04-NLS-dCas9/dCpf1-SpyTag (linker GGSGSGLQ was used), protein scaffolds 10 \times , 24 \times GCN4tag and 2 \times , 4 \times , 6 \times SpyTag were optimally synthesized by GenScript and inserted into

pIYC04-dCas9 or pIYC04-dCpf1. The corresponding protein scFv and SpyCatcher incorporating 2× NLS were also synthesized by GenScript and constructed on pJFE3 under the control of the *TEF1* promoter, a 2 μ plasmid. DNA and protein sequences were listed in Supplementary Table S5.

The plasmid pSH42H, comprising *SNR52p*, gRNA and crRNA scaffold sequences, and *SUP4t*, was used to express gRNA and crRNA, respectively. The plasmids were constructed by inverse PCR using pSH424 (28) as the template and primers containing a 20-bp sgRNA sequence. To construct multiple gRNA and crRNA arrays plasmids, individual gRNA and crRNA arrays were amplified and then assembled to pSH42H using the Golden Gate assembly method through *Bsa*I digestion and ligation. dCas9/dCpf1- and gRNA/crRNA-containing plasmids were transformed into *GFP* expression strains with different promoters to determine the efficiency of transcription regulation.

To construct strains with malonyl-CoA sensing circuits, pJfapO-fapR (29) comprising the *GAL1p(7)fapO* promoter, *eGFP*, *PGK1* terminator, and *TEF1* promoter-*fapR*, was transformed into yeast. Further, to construct strains with the ability to produce 3-HP, the gene encoding malonyl-CoA reductase (MCR) from *Chloroflexus aurantiacus* was cloned into the 2 μ plasmid pYX424 under the control of the *TEF1* promoter and *CYC1* terminator using *Bam*H/*Eco*R I digestion and ligation, followed by transformation into yeast.

gRNA design

gRNAs were designed using the Benchling website (<https://benchling.com>). As previously reported (13,30), the highest levels of activation were achieved by targeting the ~200-bp region upstream of the transcription starting site (TSS) for CRISPRa. Futher, the effect was the most prominent between the TSS and 200-bp region upstream of the TSS for CRISPRi, and gRNAs targeting either the template or non-template DNA strand for the promoter region were designed. For dCpf1, minimal off-target effect, and higher score and distribution of targeting sites were considered. Spacer sequences are listed in Supplementary Table S6. gRNAs were expressed using the *SNR52* promoter and *SUP4* terminator.

Fluorescence intensity measurement

Recombinant yeast strains were precultured at 30°C and 200 rpm, and then inoculated into fresh media (initial OD = 0.5). After culturing for approximately 12 h, cell density at OD₆₀₀ was measured using a spectrophotometer (Eppendorf BioPhotometer, Germany) and fluorescence intensity was assessed with a 1420 Multilabel Counter (Victor™ 3V, PerkinElmer, USA). GFP excitation and emission wavelengths were 485 and 528 nm, respectively. Fluorescence intensity (a.u.) was normalized to OD₆₀₀.

Flow cytometry

Cells were incubated for overnight at 30°C and 200 rpm. Mid-log phase yeast cells were then washed twice and resuspended in PBS (pH 7.0). The cultures were then diluted

to OD₆₀₀ of 1.0 and analyzed using the ImageStream Mark II imaging flow cytometer after filtering through a cell sieve to reduce aggregation. GFP fluorescence was detected with an excitation laser at 535/55 nm. Data were recorded and analyzed using IDEAS.

Quantitative RT-PCR analysis

Yeast cells were cultivated overnight and collected by centrifugation and total RNA was extracted using the UNIQ-10 Column Trizol Total RNA Isolation kit (Sangon Biotech, China) following the manufacturer's instructions. Then, the removal of gRNA and production of cDNA were performed using ReverTra Ace qPCR RT Master Mix with gDNA Remover (TOYOBO, Japan) with oligo dT primers. Quantitative PCR reactions was performed using QuantStudio 3 Real-Time PCR Instrument (Thermo Fisher Scientific) with SYBR Green-based method. Actin and Tub1 were internal reference gene, and primer sequences are listed in Supplementary Table S7.

Transcriptome analysis

Yeast cells were cultured to the mid-exponential phase (OD₆₀₀ ≈ 1), centrifuged, and frozen in liquid nitrogen. Total RNA of the yeast was extracted by UNIQ-10 TRIzol RNA purification kit (Sangon Biotech, China). mRNA was enriched and rRNA was removed from total RNA. RNA was fragmented into fragments, and single-stranded circular DNA libraries were constructed using PCR. The library was sequenced by Illumina HiSeq 2500 (performed by Beijing Genomics Institute) with paired ends (2 × 125 bp) according to the manufacturer's instructions. The clean reads obtained by data filtering were mapped to the reference genome of CEN.PK113-7D (<https://www.yeastgenome.org/strain/S000203459>), with an average of 87.7% of the reads being successfully mapped. Analysis of the differentially expressed genes (DEGs) was carried out in R using the DEGs package. Corrected P value <0.05 and absolute |log₂FC| > 1 were set as the threshold for significantly changed genes. All annotations were derived from the SGD (<http://www.yeastgenome.org/>). All analyses were performed in biological triplicates.

3-HP production and quantification

For 3-HP production, cells were precultured in SC-HIS3-URA3/HygB media for ~2 days; they were then inoculated into 40 mL media (initial OD₆₀₀ = 0.2) and cultured at 30°C and 200 rpm for 72 h. 3-HP levels were determined by HPLC (Shimadzu Corporation, Japan) with an Aminex HPX-87H column (Bio-Rad, Hercules, United States) at 65°C. The mobile phase was 2.5 mM H₂SO₄ and the flow rate was 0.6 ml/min (31).

Data analysis

The gene activation and repression were expressed as activation fold or repression ratio by calculating the ratio between the fluorescence intensity of the reporter with gRNA expression and the fluorescence intensity of the reporter without gRNA. The biological triplicates were performed and

error bars represent the means \pm standard deviation (SD) from biological triplicates.

RESULTS

Evaluation of the activation domain for CRISPR activation

Activator strength is the most important factor affecting the activation. To evaluate transcription activator performance, *GFP* driven by the *LEU2* promoter was inserted into the *TRP1* locus. VP64-p65-Rta, a tripartite activator VPR system, is a frequently used for CRISPR transcription hybrid activator and the activation efficiency was shown to be better than VP64 (6). In our previous study, we found that the subunit of the RNA polymerase II mediator complex Med2 could also activate gene expression and that the activation efficiency was higher than that of VPR and endogenous activator Gal4 on fusion with a prokaryotic transcription factor in *S. cerevisiae* (32). We therefore fused VPR, Med2, and truncated Med2 (aa156–258 + aa380–431, dMed2), which only contains the activation domain of Med2 (33), with dCas9 from *Streptococcus pyogenes*, followed by comparison of activation efficiencies (Figure 1A). We found that dCas9-VPR activated the expression by 2.1-fold, and dCas9-dMed2 showed similar activation efficiency. Further, dCas9-Med2 demonstrated the highest activation efficiency; dCas9-Med2 activated the expression by 2.8-fold, which was 29.5% higher than that shown by dCas9-VPR (Figure 1A). These findings indicated that Med2 indeed showed better activation efficiency than VPR.

Creation of protein scaffolds to enhance CRISPR-mediated activation

Gene transcription level is strongly regulated by the copy number of transcription factors that is recruited to the promoters (11,34). To assess the effect of recruiting multiple copies of transcriptional regulators, two protein scaffolds SunTag and SPY systems were introduced in the CRISPRa system. The SunTag system (14), consists of 10 or 24 copies of the 19 residue GCN4 peptide and a single-chain variable fragment (scFv) of the anti-GCN4 antibody as a tag.

The GCN4 peptide were fused with dCas9 via a GGGSGGGGS linker (Figure 1B). For efficient nuclear import, one SV40 nuclear localization signal (NLS) was inserted in the N-terminal of dCas9 and two NLSs were inserted in the N-terminal of SunTag, similar to a previously reported design (14). dCas9-SunTag could recruit multiple scFv-Med2 fusion proteins via antigen–antibody interactions. On activation efficiency assessment, we found that dCas9-Med2 activated the expression of *GFP* driven by the *LEU2* promoter by 2.8-fold, whereas dCas9-10 × SunTag and dCas9-24 × SunTag activated the expression by 4.2- and 3.6-fold, respectively, with these values being 46% and 27% higher than that shown by dCas9-Med2, respectively. These data validated that the SunTag system was able to successfully amplify activation efficiency (Figure 1B). However, the activation efficiency of dCas9-24xSunTag appeared to be lower than that of dCas9-10xSunTag. Similar to our work, a previous study reported that dCas9-10xSunTag was shown to have a similar maximal activa-

tion in gene expression compared with dCas9-24xSunTag (14). Herein, although dCas9-SunTag-Med2 system amplified the activation, comparing with dCas9-Med2, the improvement is not very significant.

We then evaluated whether Spycatcher/Spytag can function in the CRISPR regulation system. Considering that the application of Spycatcher/Spytag in *S. cerevisiae* has not been previously reported, we first determined the effect of Spycatcher/Spytag. The dCas9 was fused with SpyTag via a GGSGSGLQ linker (Figure 1C). One and two SV40 nuclear localization signal (NLS) was inserted in the N-terminal of dCas9 and SpyTag, respectively, to ensure efficient nuclear import. 2, 4 or 6 copies of repeated SpyTag were fused with dCas9 and Med2 was fused with SpyCatcher. We found that dCas9-SPY activated the expression of *GFP* by 6.9-, 6.4- and 7.9-fold, respectively. In comparison with dCas9-Med2, the activation efficiency of dCas9-6 × SPY was 3.3-fold higher (Figure 1C). These results were consistent with the flow cytometry data (Figure 1D). These findings demonstrated that both SunTag and Spycatcher/Spytag amplified the activation efficiency of CRISPR-mediated gene expression, and the Spycatcher/Spytag system was more effective than the SunTag system.

To demonstrate the applicability of Spycatcher/Spytag (Figure 2A), we then investigated the activation efficiency on *GAL7*, *HED1* and *CYC1* promoters. dCas9-2 × SPY or dCas9-6 × SPY was found to activate gene expression by 34.9-, 20.7-, and 3.6-fold, respectively, and these values were 3.8-, 4.4- and 4.1-fold higher than those shown by dCas9-Med2, respectively (Figure 2B–D). The transcriptional level was also correlated with the change of fluorescence (Figure 2E). The dCas9-2 × SPY and dCas9-6 × SPY systems thus exhibited good activation efficiencies as well as applicability with different promoters.

dCas9-mediated repression signal amplification system

Basis the aforementioned results, we subsequently constructed a CRISPRi signal amplification system. As SpCas9 has been well characterized in yeast (7), we compared the transcription repression efficiency of dCas9-TUP1 (domain of TUP1, 73–129 aa) and dCas9/TUP1 combined the Spytag/Spycatcher or SunTag system. The yeast general repressor protein TUP1 represses transcription by forming a complex with Ssn6; the Ssn6–Tup1 complex is regarded as a global repressor considering its ability to repress multiple families of genes (7,35,36). With the *HHF2* promoter, we observed that dCas9-TUP1 repressed the expression by only 38%, and both the CRISPRi signal amplification systems showed higher repression abilities than dCas9-TUP1. dCas9-24 × SunTag and dCas9-6 × SPY showed better repression efficiency, repressing *GFP* expression by 73% and 63%, respectively, being 2.2- and 1.6-fold higher than that shown by dCas9-TUP1 (Figure 3). These results indicated both the CRISPR-mediated SunTag and SPY systems achieved better repression than dCas9-TUP1, with the 24 × SunTag system showing the best repression effect. The dCas9-SunTag system also worked effectively with other promoters (e.g. *PGK*) (Supplementary Figure S1).

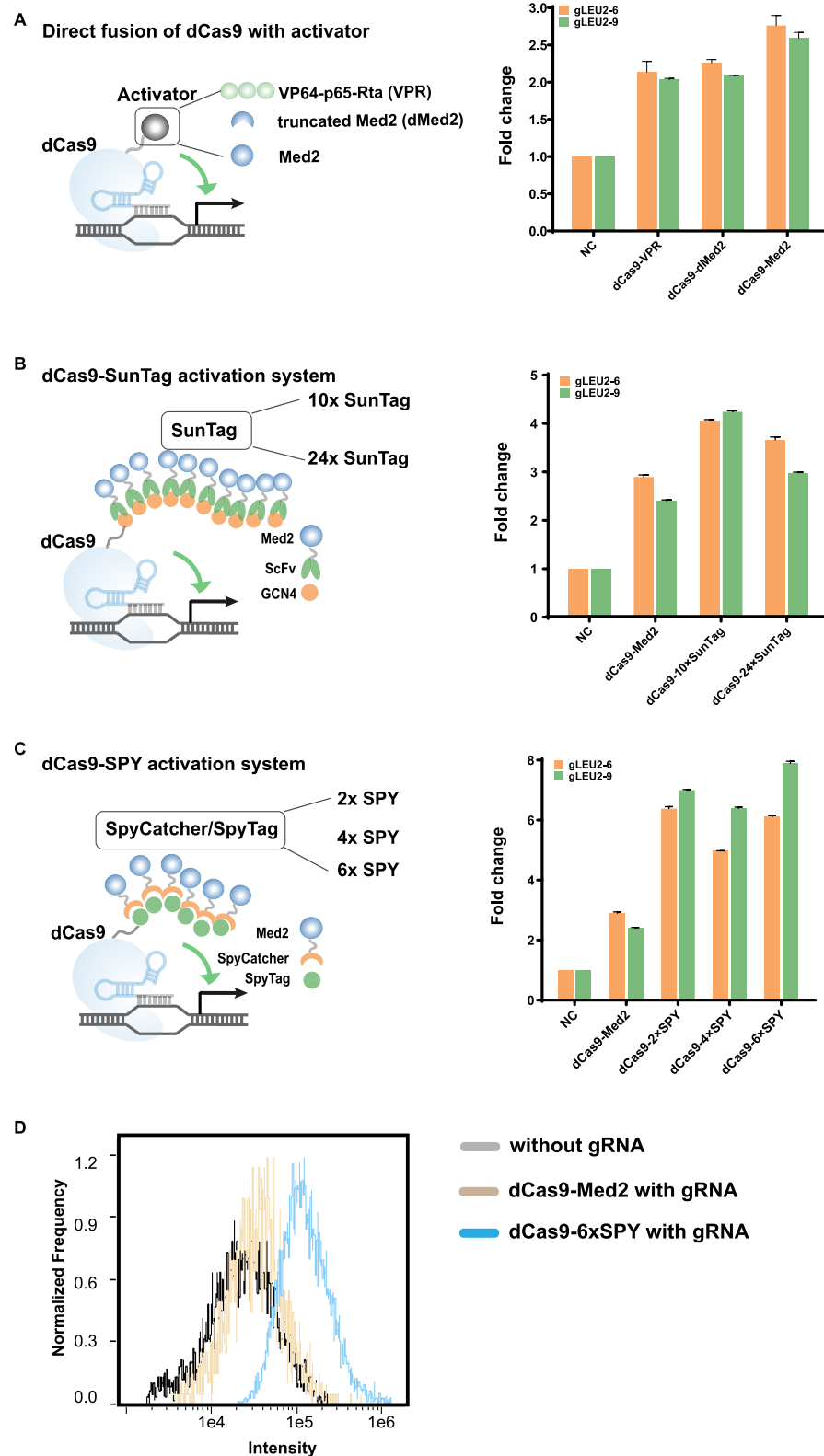


Figure 1. Optimization of CRISPR-based regulator recruiting systems for gene activation. (A) Activation efficiency of the activation domain fused with dCas9. (B) Activation efficiency of dCas9 and activation domain (Med2) with different SunTag and (C) SPY systems. (D) Flow cytometry results pertaining to strains expressing dCas9-Med2 or dCas9-6 × SPY with gLEU2-9 gRNA. NC: control strains without gRNA. Values represent mean ± standard deviation of three independent experiments.

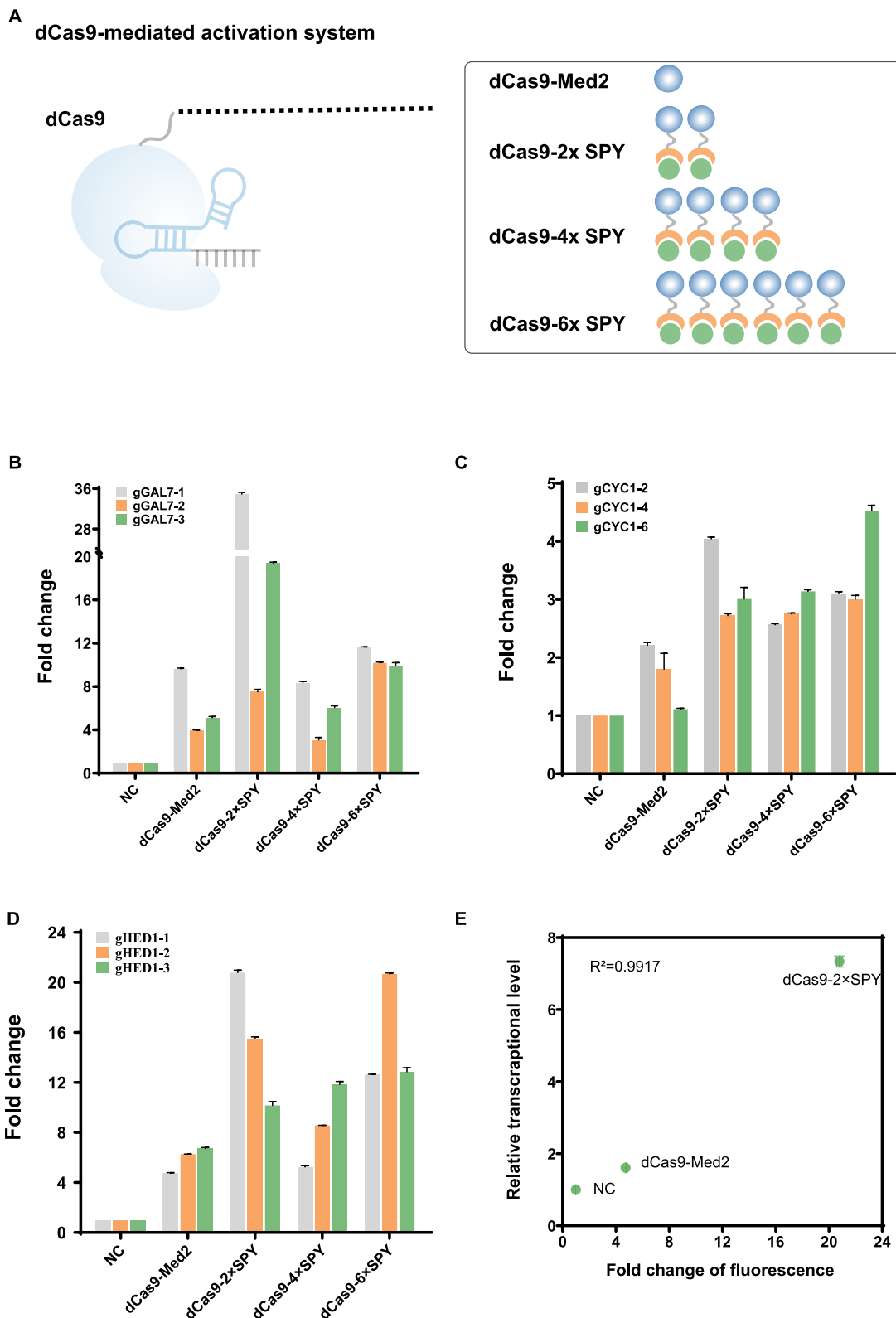


Figure 2. Activation efficiency of dCas9-SPY-Med2 using different promoters. (A) Schematic of dCas9-mediated activation system. Data pertaining to (B) *GAL7*, (C) *CYC1* and (D) *HED1* promoters. (E) The correlation of fold change of fluorescence and relative transcriptional level using gHED1-1 gRNA.

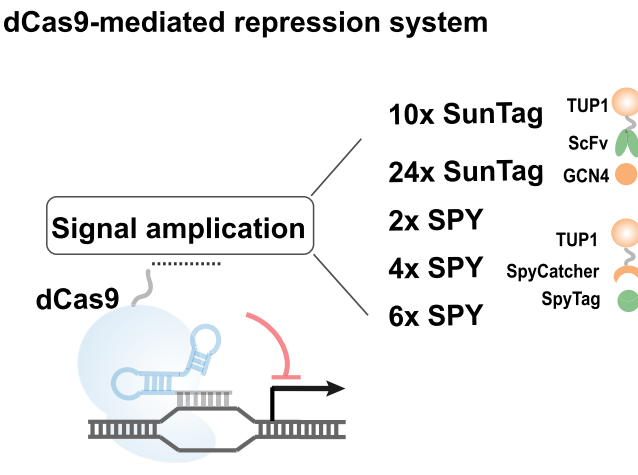
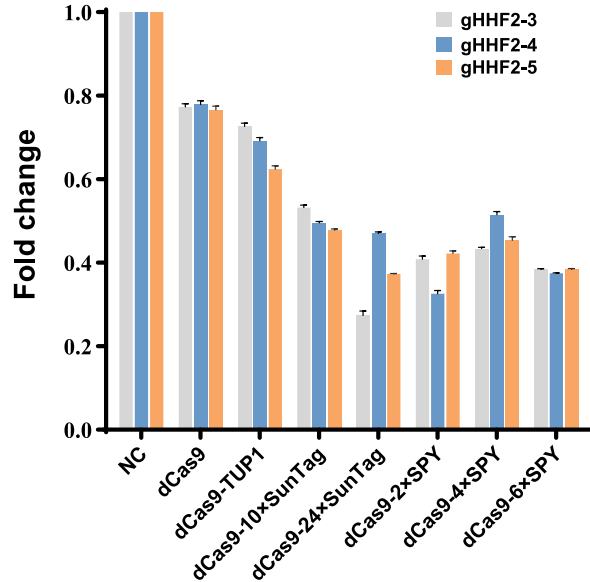


Figure 3. Comparison of dCas9-based regulator recruiting systems for gene interference. Repression efficiency of the dCas9-SunTag and dCas9-SPY systems with the repression domain TUP1.

Construction of an efficient orthogonal bifunctional CRISPR-mediated transcriptional regulation system

To develop an orthogonal bifunctional CRISPR-mediated transcriptional regulation system, nuclease-deficient CRISPR proteins that can recognize different PAM sequences are required. dCpf1 from *Lachnospiraceae bacterium* ND2006, favoring 5'-TTTV-3' PAM sequences (dCpf1), has been characterized (37) and used for CRISPR regulation or genome editing in *S. cerevisiae* (38,39). We thus chose dCpf1 to construct an orthogonal bifunctional CRISPR-mediated transcriptional regulation system. Considering the high activation efficiency shown by dCas9-SPY, we built a gene repression system orthogonal to dCas9-SPY. dCpf1-SunTag-TUP1 was constructed and its inhibitory effect was determined. However, although the repression efficiency of dCpf1-10 × SunTag-TUP1 and dCpf1-24 × SunTag-TUP1 were higher than that of dCpf1-TUP1, only 43% and 44% repression was achieved, respectively (Supplementary Figure S2), and flow cytometry results also confirmed the differences of repression efficiency of dCpf1-TUP1, dCpf1-10 × SunTag-TUP1 and dCpf1-24 × SunTag-TUP1 is not very big (Supplementary Figure S3). To improve repression efficiency, we evaluated and compared the inhibitory effects of the repression domains of TUP1, Mxi1 and MIG1 (4,7,40). dCpf1-Mix1 and dCpf1-MIG1 showed better repression efficiency than dCpf1-TUP1, which is consistent with previous findings (4) and both downregulated GFP expression by approximately 50% for HHF2 promoter (Figure 4A). The repression ratio of dCpf1-MIG1 can reach to 70% when targeting to ENO2 promoter (Supplementary Figure S4). We then selected MIG1 as the repression domain to establish a repressor recruiting system. Relative to dCpf1-MIG1, dCpf1-10 × SunTag and dCpf1-24 × SunTag showed much higher inhibition of GFP expression, reaching up to 77% and 76%, respectively (Figure 4B). Flow cytometry results



showed similar trend (Figure 4C). We also examined the repression of GFP expression driven by the ENO2 and ENO1 promoters from *Kluyveromyces lactis* (Figure 5A–C). The repression efficiency can reach to 95% and 86%, respectively, using dCpf1-24 × SunTag-MIG1, being 7.9- and 2-fold higher than that shown by dCpf1-MIG1, respectively (Figure 5B and C). The transcriptional level was also down-regulated significantly by dCpf1-24 × SunTag-MIG1 and it is correlated with the change of fluorescence (Figure 5D). These findings demonstrated that highly efficient repression could be achieved by dCpf1-24 × SunTag.

To verify the orthogonality of the two CRISPR-mediated systems, a strain containing two reporter proteins was constructed: eGFP driven by the HHF2 promoter and mKate driven by the LEU2 promoter were inserted into the TRP1 and LEU2 locus, respectively. The dCas9-SPY- and dCpf1-SunTag-containing plasmids were then transformed into the strain to simultaneously regulate mKate and eGFP expression. mKate expression was upregulated by 3.2-fold and eGFP expression was downregulated by 69%, comparable to the single CRISPR-mediated system (Supplementary Figure S5). This indicated that the two CRISPR-mediated systems were orthogonal, with no crosstalk between them.

Combinatorial regulation of 3-HP production using CRISPRa/i signal amplification systems

To detect CRISPRa/i orthogonality and application, as a proof-of-concept study, we used CRISPRa/i signal amplification systems to regulate the metabolic pathway responsible for 3-HP production. 3-HP, a non-chiral, optically inactive, three-carbon molecule, is one of the top 12 value-added chemicals from biomass selected by the US Department of Energy (41). 3-HP is produced from glucose with malonyl-CoA as an intermediate via the catalysis of MCR, a bifunctional enzyme from *Chloroflexus aurantiacus* (Figure 6A) (31,42). Malonyl-CoA is synthesized by acetyl-

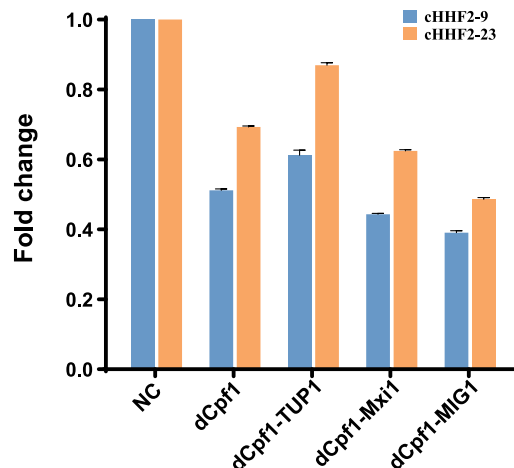
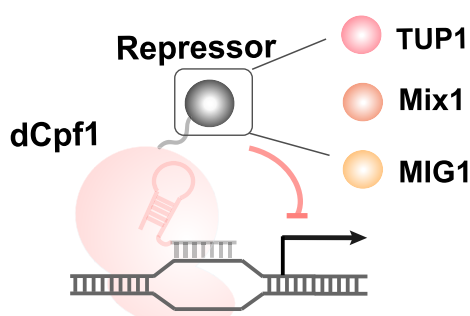
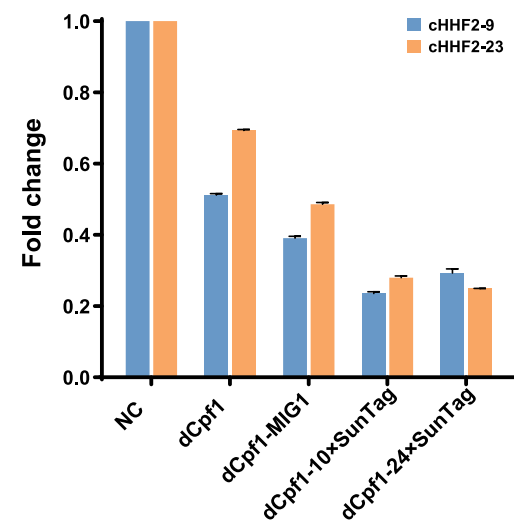
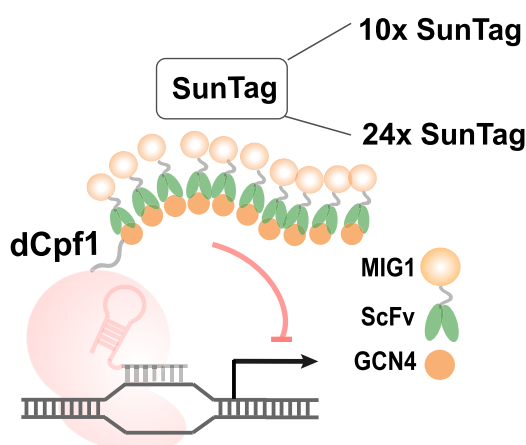
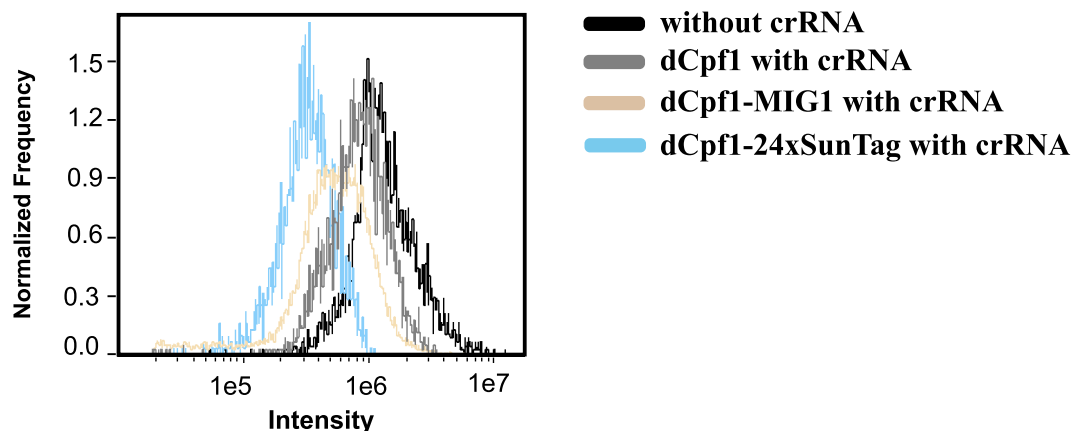
A Direct fusion of dCpf1 with repressor**B dCpf1-SunTag repression system****C**

Figure 4. Optimization of dCpf1-based CRISPR regulator recruiting systems for gene repression. (A) Repression efficiency of the activation domain fused with dCpf1. (B) Repression efficiency of dCpf1 and repression domain (MIG1) with different SunTag systems. (C) Flow cytometry results pertaining to strains expressing dCpf1, dCpf1-MIG1 and dCpf1-24 × SunTag with cHHF2-23 crRNA.

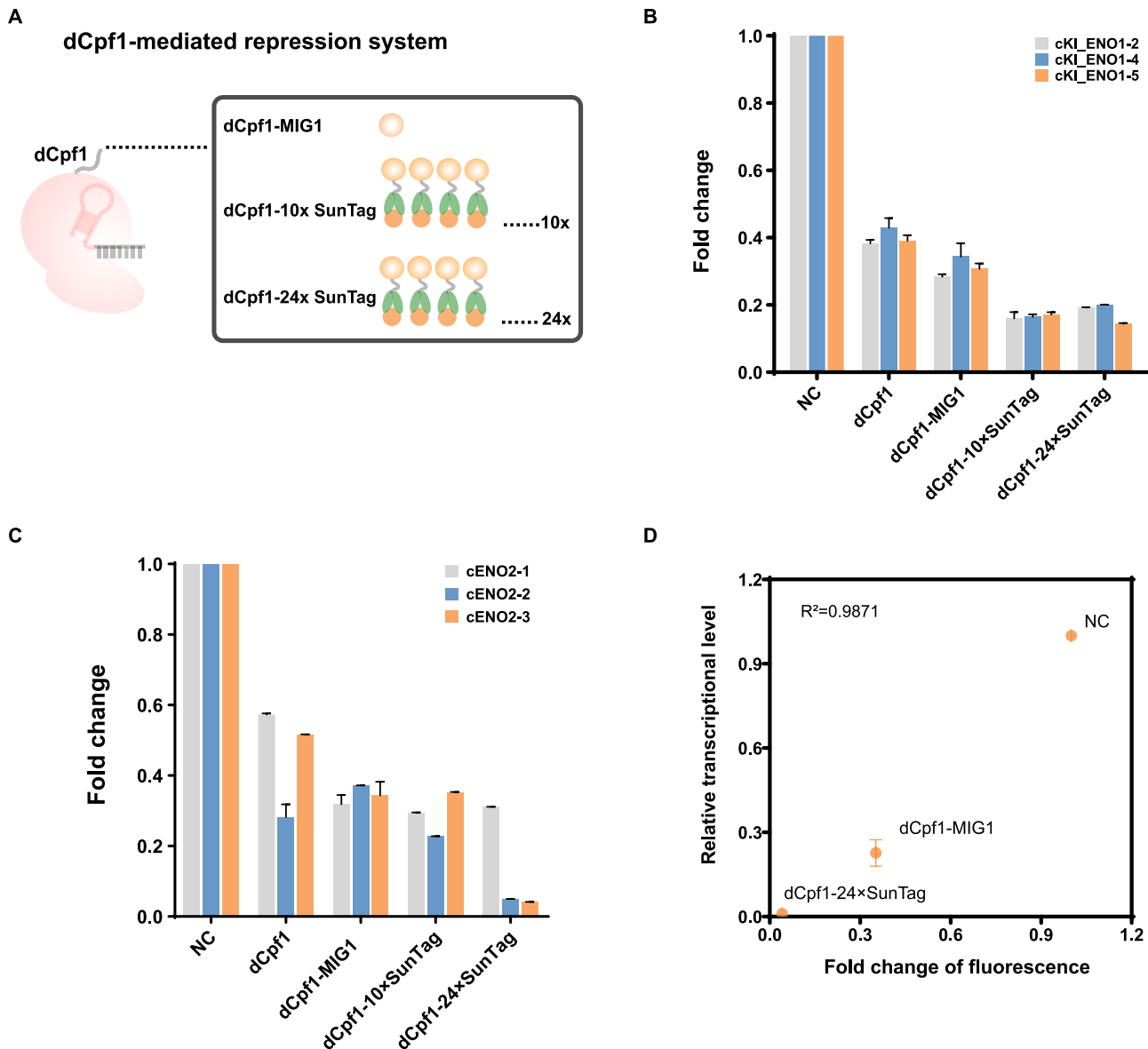


Figure 5. Repression efficiency of dCpf1-SunTag using different promoters. (A) Schematic of dCpf1-mediated repression system. (B) The dCpf1-SunTag system combining the repression domain MIG1 targeting *Kl-ENO1* from *K. lactis* and (C) *ENO2* promoter. (D) The correlation of fold change of fluorescence and relative transcriptional level with *ENO2* promoter using cENO2-1 crRNA.

CoA carboxylase (*Acc1*) and is essentially used for fatty acid synthesis. Malonyl-CoA availability directly affects 3-HP production; therefore, it is important to increase the synthesis of malonyl-CoA and decrease its consumption in the cytoplasm. *ACC1* overexpression can evidently increase 3-HP production (43). Furthermore, the fatty acid synthetase system (*FAS1*/*FAS2*) catalyzes the synthesis of long-chain saturated fatty acids using malonyl-CoA as a substrate (44,45). Therefore, we first chose these genes as targets for CRISPR regulation. In addition to 3-HP production, we detected malonyl-CoA availability using our previously constructed malonyl-CoA biosensor (fapO/fapR system) to control *eGFP* expression (Figure 6A) (29). *FAS1*/*FAS2* repression increased malonyl-CoA availability. Individually repressing *FAS1* or *FAS2* using dCpf1-

SunTag-TUP1, the fluorescence intensity was observed to increase by 24.1- and 30.0-fold, respectively. Simultaneously repressing *FAS1* and *FAS2* enhanced the fluorescence intensity by 33.0-fold, whereas only 2.6-fold increase in the fluorescence intensity was detected on using dCpf1-TUP1 to inhibit *FAS1* and *FAS2* (Figure 6B). In comparison to using dCas9-Med2 for activating *ACC1* expression, dCas9-6 × SPY showed better activation efficiency, as the fluorescence intensity of the malonyl-CoA biosensor was 2.2-fold higher than that in the dCas9-Med2 strain (Figure 6C). Furthermore, when using dCas9-Med2, we did not observe any obvious increase in 3-HP production levels; while 3-HP production levels were improved by 31% when dCas9-6 × SPY was used to activate *ACC1* expression (Figure 6D). Similarly, 3-HP production level was improved by 55% when

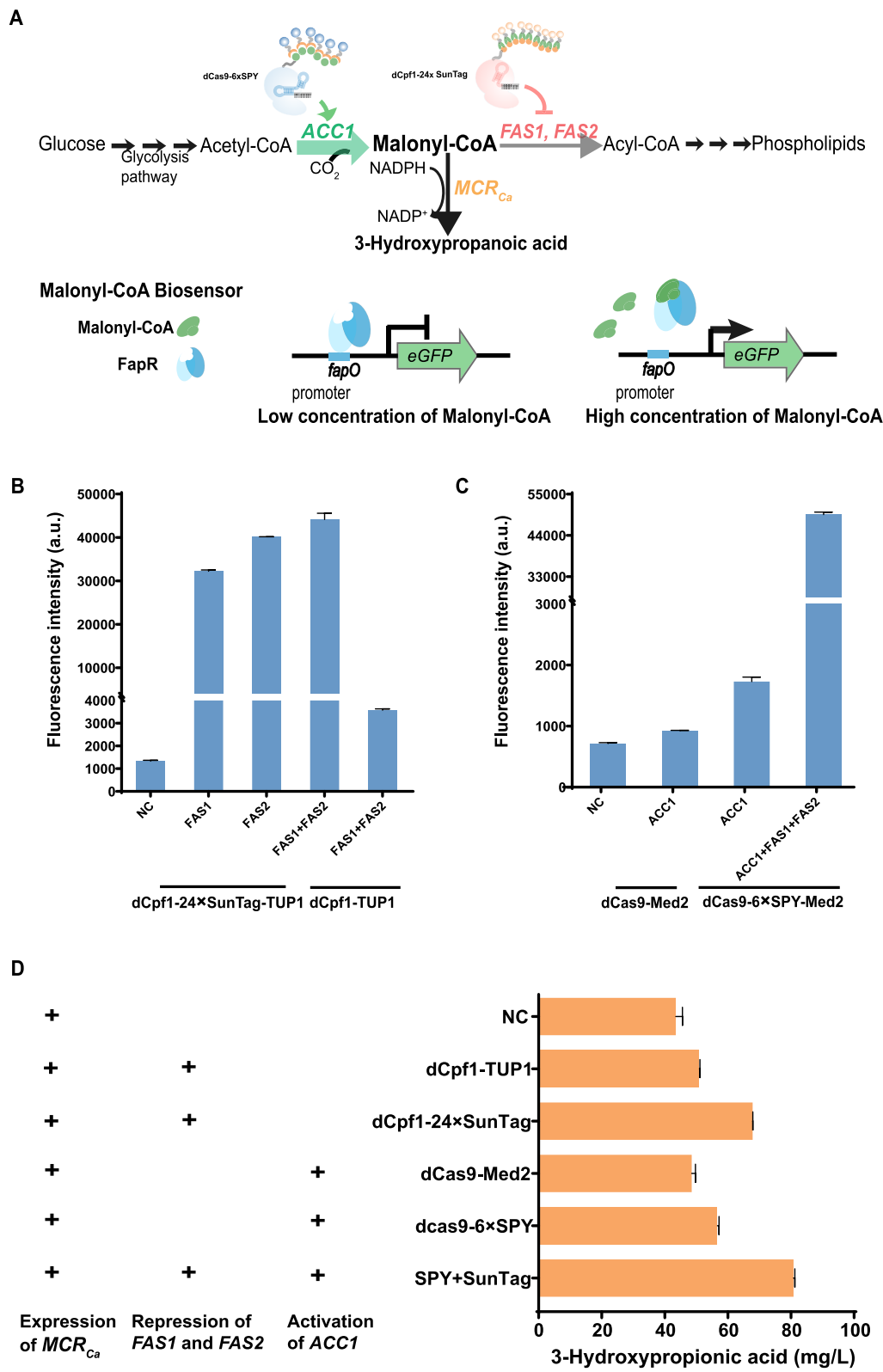


Figure 6. Simultaneous up- and downregulation of pertinent genes to improve 3-HP production using CRISPR-mediated regulator recruiting systems. (A) 3-HP biosynthesis pathway and biosensor design in *S. cerevisiae*. *ACC1* and *FAS1/FAS2* were chosen to be up- and downregulated using the dCas9-SPY and dCpf1-SunTag systems, respectively. A biosensor was used to detect malonyl-CoA availability. FapR bound to the *fapO* site to prevent transcription of downstream genes. With an increase in malonyl-CoA levels, FapR bound to malonyl-CoA, dissociating from the *fapO* site and upregulating transcription levels. (B) Fluorescence intensity of malonyl-CoA biosensor in the strain with *FAS1* and *FAS2* repression and (C) with *ACC1* upregulation or with simultaneous *FAS* down- and *ACC1* up-regulation. (D) 3-HP accumulation in strains with simultaneous up- and downregulation of different genes. '+': gene was expressed, activated or repressed.

dCpf1-24 × SunTag-TUP1 was used to repress *FAS1* and *FAS2*, which was 35% higher than the improvement observed on using dCpf1-TUP1 (Figure 6D). We found that the repression of *FAS1/FAS2* by dCpf1-SunTag-MIG1 produces a higher level of 3-HP than dCpf1-SunTag-TUP1, but it decreased the growth significantly (Supplementary Figure S6). Considering that significant downregulation of *FAS1/FAS2* have negative impact to cell growth, here we used dCpf1-24 × SunTag-TUP1 for *FAS1/FAS2* regulation.

To determine if a combinatorial effect was achievable by CRISPRa/i systems, simultaneous upregulation of *ACCI* and downregulation of *FAS1* and *FAS2* were performed (SPY + SunTag) (Figure 6C and D). Compared to when only *FAS1* and *FAS2* expression was repressed, the fluorescence intensity of the malonyl-CoA biosensor was 1.1-fold higher and 3-HP production level was further increased by 19%. In addition to *ACCI*, *FAS1* and *FAS2*, we also performed simultaneous regulation *ARG3* gene. Arg3 is associated with the biosynthesis of the arginine precursor citrulline, and our recent study has reported that the deletion of *ARG3* increased the accumulation of 3-HP (46). The results showed that combining *FAS1*, *FAS2* and *ARG3* downregulation and *ACCI* upregulation, the production of 3-HP was further increased by 16%, demonstrated the advantage of our CRISPR-based system (Supplementary Figure S7).

DISCUSSION

S. cerevisiae is a very important microbial cell factory for produce numerous chemicals (47,48). Although CRISPR system has been developed for gene regulation in yeast and high regulation levels have been achieved for some specific promoters, the regulation efficiency remains relatively low for many genes when using either single or few activators or repressors. In the present study, we established two CRISPR-mediated transcriptional regulation systems that recruited multiple copies of regulators for efficient transcription programming. Gene activation and repression abilities were significantly increased irrespective of the choice of promoters. Gene expression was activated by as high as 34.9-fold and the repression efficiency as much as 95%, with these values being 3.8- and 8.6-fold higher than those observed on the direct fusion of regulators with nuclease-deficient CRISPR proteins, respectively. These data demonstrated that the CRISPR-mediated regulator recruiting system is a powerful, robust tool to amplify regulator efficiency.

SunTag in combination with CRISPR has been applied for gene editing, gene regulation, DNA methylation or demethylation, and RNA demethylation in mammalian cells and plants (19–22,49,50), its application in yeast has not been reported. Moreover, orthogonal CRISPR-mediated protein-tagging activation and repression systems have not been developed as yet. Although SPY has been widely used for protein assembly (15,25), the effects of different numbers of SpyCatcher/SpyTag for CRISPR-mediated signal amplification remain to be determined. Herein the SpyCatcher/SpyTag protein scaffolds were used and systematically compared for CRISPR-mediated signal amplification for the first time. We found that tag number

was not positively correlated with regulation efficiency. In the SPY system, 2 and 6 copies of repeated SpyCatcher were more effective than 4 copies, with the regulation efficiency being much better than that of 10× or 24× SunTag. Besides, in the SunTag system, 10 copies of the GCN4 peptide showed higher activation efficiency, while 24 copies of the GCN4 peptide showed better gene repression ability. It is still unclear how regulators that are recruited to the promoter region can achieve the highest regulation level. It appears that the efficiency is affected by various factors, such as promoter characteristics and location and binding affinity of gRNA/crRNA. We also performed transcriptome analysis to determine impact of this system on global gene expression and found that the expression of a small number of endogenous genes were altered regardless whether they contained dCas-TFs or CRISPR-based signal amplification systems (Supplemental Figures 8, 9 and Supplemental RNAseq Data). When using different gRNA, the significantly changed genes were also changed. We speculated that this may be caused by off-targeting of the dCas proteins.

Previously, the activation efficiency based on dCas9-VPV and the inhibition efficiency based on dCpf1-Mx1 can reach to 4.5~12-fold and 75%~95%, respectively, for different promoter in *S. cerevisiae* (7,38). Here, we compared the regulation efficiency of transcription factors and coupled the transcription factors with SPY and Sun Tag systems. The optimized dCas9-SPY and dCpf1-SunTag regulation systems are able to achieve 3.6~34.9-fold activation and near-complete repression, respectively, on promoters of different strengths. This suggests that the signal amplification system we have constructed further refines the gene regulation tools in *S. cerevisiae*. As anticipated, different repression or activation domains showed different repression or activation efficiencies, respectively. Ciurkot *et al.* recently demonstrated that Mx1 and MIG1 enabled better downregulation relative to other repression domains (37,38). Our result was consistent with their finding, as even we found that the repression efficiency of MIG1 and Mx1 was better than that of TUP1. In addition, we found that Med2 showed better activation efficiency than VPR. Med2 is a component of the mediator complex, and its presence may result in the recruitment of mediator and other core components of the transcription machinery more directly, consequently leading to better activation efficiency. Based on the optimization of transcription effectors, protein scaffolds, and CRISPR proteins, an effective orthogonal CRISPR-mediated system should comprise dCas9-SPY-Med2 for transcriptional activation and dCpf1-SunTag-MIG1 for transcriptional interference. Finally, as a proof-of-concept study, we demonstrated that our orthogonal system was stably maintained and that combinatorial regulation of 3-HP production was achievable via orthologous regulation of gene expression.

To summarize, we developed and optimized two CRISPR-mediated signal amplification systems in *S. cerevisiae*, which showed good orthogonality and significantly amplified regulatory signals. Then we assembled these two CRISPR modules together and applied them to regulate a metabolic pathway. This system considerably improved gene regulation efficiency, and thus, we believe it should be valuable for both metabolic engineering and fundamental studies.

DATA AVAILABILITY

All data generated or analyzed during this study are included in this published article and its supplementary information files. RNAseq raw data are submitted to the NCBI Sequence Read Archive under the BioProjects: PRJNA825362 and PRJNA827973.

SUPPLEMENTARY DATA

[Supplementary Data](#) are available at NAR Online.

ACKNOWLEDGEMENTS

We would like to thank Jingyao Qu and Yan Wang from State Key laboratory of Microbial Technology of Shandong University for assistance in flow cytometry.

FUNDING

National Key R&D Program of China [2021YFC2100500]; National Natural Science Foundation of China [31970082]; Key R&D Program of Shandong Province [2020CXGC010602]; National Natural Science Foundation of Shandong Province [ZR2020YQ18]. Funding for open access charge: National Key R&D Program of China [2021YFC2100500].

Conflict of interest statement. None declared.

REFERENCES

- Steen,E.J., Chan,R., Prasad,N., Myers,S., Petzold,C.J., Redding,A., Ouellet,M. and Keasling,J.D. (2008) Metabolic engineering of *Saccharomyces cerevisiae* for the production of n-butanol. *Microb. Cell Fact.*, **7**, 36.
- Shiba,Y., Paradise,E.M., Kirby,J., Ro,D.K. and Keasling,J.D. (2007) Engineering of the pyruvate dehydrogenase bypass in *saccharomyces cerevisiae* for high-level production of isoprenoids. *Metab. Eng.*, **9**, 160–168.
- Qi,L.S., Larson,M.H., Gilbert,L.A., Doudna,J.A., Weissman,J.S., Arkin,A.P. and Lim,W.A. (2013) Repurposing CRISPR as an RNA-guided platform for sequence-specific control of gene expression. *Cell*, **152**, 1173–1183.
- Gilbert,L.A., Larson,M.H., Morsut,L., Liu,Z., Brar,G.A., Torres,S.E., Stern-Ginossar,N., Brandman,O., Whitehead,E.H., Doudna,J.A. *et al.* (2013) CRISPR-mediated modular RNA-guided regulation of transcription in eukaryotes. *Cell*, **154**, 442–451.
- Maeder,M.L., Linder,S.J., Cascio,V.M., Fu,Y., Ho,Q.H. and Joung,J.K. (2013) CRISPR RNA-guided activation of endogenous human genes. *Nat. Methods*, **10**, 977–979.
- Chavez,A., Scheiman,J., Vora,S., Pruitt,B.W., Tuttle,M., E.P.R.Iyer., Lin,S., Kiani,S., Guzman,C.D., Wiegand,D.J. *et al.* (2015) Highly efficient Cas9-mediated transcriptional programming. *Nat. Methods*, **12**, 326–328.
- Lian,J., HamedRad,M., Hu,S. and Zhao,H. (2017) Combinatorial metabolic engineering using an orthogonal tri-functional CRISPR system. *Nat. Commun.*, **8**, 1688.
- Edmondson,D.G., Smith,M.M. and Roth,S.Y. (1996) Repression domain of the yeast global repressor TUP1 interacts directly with histones H3 and H4. *Genes Dev.*, **10**, 1247–1259.
- Ostling,J., Carlberg,M. and Ronne,H. (1996) Functional domains in the mig1 repressor. *Mol. Cell. Biol.*, **16**, 753–761.
- Kadosh,D. and Struhl,K. (1997) Repression by ume6 involves recruitment of a complex containing sin3 corepressor and rpd3 histone deacetylase to target promoters. *Cell*, **89**, 365–371.
- Pettersson,M. and Schaffner,W. (1990) Synergistic activation of transcription by multiple binding sites for NF-kappa B even in absence of co-operative factor binding to DNA. *J. Mol. Biol.*, **214**, 373–380.
- Zalatan,J.G., Lee,M.E., Almeida,R., Gilbert,L.A., Whitehead,E.H., La Russa,M., Tsai,J.C., Weissman,J.S., Dueber,J.E., Qi,L.S. *et al.* (2015) Engineering complex synthetic transcriptional programs with CRISPR RNA scaffolds. *Cell*, **160**, 339–350.
- Konermann,S., Brigham,M.D., Trevino,A.E., Joung,J., Abudayyeh,O.O., Barcena,C., Hsu,P.D., Habib,N., Gootenberg,J.S., Nishimasu,H. *et al.* (2015) Genome-scale transcriptional activation by an engineered CRISPR-Cas9 complex. *Nature*, **517**, 583–588.
- Tanenbaum,M.E., Gilbert,L.A., Qi,L.S., Weissman,J.S. and Vale,R.D. (2014) A protein-tagging system for signal amplification in gene expression and fluorescence imaging. *Cell*, **159**, 635–646.
- Ma,D., Peng,S., Huang,W., Cai,Z. and Xie,Z. (2018) Rational design of mini-cas9 for transcriptional activation. *ACS Synth. Biol.*, **7**, 978–985.
- Ji,H., Jiang,Z., Lu,P., Ma,L., Li,C., Pan,H., Fu,Z., Qu,X., Wang,P., Deng,J. *et al.* (2016) Specific reactivation of latent HIV-1 by dCas9-SunTag-VP64-mediated guide RNA targeting the HIV-1 promoter. *Mol. Ther.*, **24**, 508–521.
- Papikian,A., Liu,W., Gallego-Bartolomé,J. and Jacobsen,S.E. (2019) Site-specific manipulation of arabidopsis loci using CRISPR-Cas9 suntag systems. *Nat. Commun.*, **10**, 729.
- Jiang,W., Feng,S., Huang,S., Yu,W., Li,G., Yang,G., Liu,Y., Zhang,Y., Zhang,L., Hou,Y. *et al.* (2018) BE-PLUS: a new base editing tool with broadened editing window and enhanced fidelity. *Cell Res.*, **28**, 855–861.
- Gallego-Bartolome,J., Gardiner,J., Liu,W., Papikian,A., Ghoshal,B., Kuo,H.Y., Zhao,J.M., Segal,D.J. and Jacobsen,S.E. (2018) Targeted DNA demethylation of the arabidopsis genome using the human TET1 catalytic domain. *Proc. Natl. Acad. Sci. U.S.A.*, **115**, E2125–E2134.
- Morita,S., Noguchi,H., Horii,T., Nakabayashi,K., Kimura,M., Okamura,K., Sakai,A., Nakashima,H., Hata,K., Nakashima,K. *et al.* (2016) Targeted DNA demethylation in vivo using dCas9-peptide repeat and scFv-TET1 catalytic domain fusions. *Nat. Biotechnol.*, **34**, 1060–1065.
- Huang,Y.H., Su,J., Lei,Y., Brunetti,L., Gundry,M.C., Zhang,X., Jeong,M., Li,W. and Goodell,M.A. (2017) DNA epigenome editing using CRISPR-Cas suntag-directed DNMT3A. *Genome Biol.*, **18**, 176.
- Zhang,X., Wang,W., Shan,L., Han,L., Ma,S., Zhang,Y., Hao,B., Lin,Y. and Rong,Z. (2018) Gene activation in human cells using CRISPR/Cpf1-p300 and CRISPR/Cpf1-SunTag systems. *Protein Cell*, **9**, 380–383.
- Li,L., Fierer,J.O., Rapoport,T.A. and Howarth,M. (2014) Structural analysis and optimization of the covalent association between spycatcher and a peptide tag. *J. Mol. Biol.*, **426**, 309–317.
- Reddington,S.C. and Howarth,M. (2015) Secrets of a covalent interaction for biomaterials and biotechnology: spytag and spycatcher. *Curr. Opin. Chem. Biol.*, **29**, 94–99.
- Qu,J., Cao,S., Wei,Q., Zhang,H., Wang,R., Kang,W., Ma,T., Zhang,L., Liu,T., Wing-Ngor Au,S. *et al.* (2019) Synthetic multienzyme complexes, catalytic nanomachineries for cascade biosynthesis in vivo. *ACS Nano*, **13**, 9895–9906.
- Engler,C. and Marillonnet,S. (2014) Golden gate cloning. *Methods Mol. Biol.*, **1116**, 119–131.
- Farzadfar,F., Perli,S.D. and Lu,T.K. (2013) Tunable and multifunctional eukaryotic transcription factors based on CRISPR/Cas. *ACS Synth Biol.*, **2**, 604–613.
- Zhang,G.C., Kong,II., Kim,H., Liu,J.J., Cate,J.H. and Jin,Y.S. (2014) Construction of a quadruple auxotrophic mutant of an industrial polyploid *saccharomyces cerevisiae* strain by using RNA-guided cas9 nuclease. *Appl. Environ. Microbiol.*, **80**, 7694–7701.
- Chen,X., Yang,X., Shen,Y., Hou,J. and Bao,X. (2018) Screening phosphorylation site mutations in yeast acetyl-CoA carboxylase using malonyl-CoA sensor to improve malonyl-coa-derived product. *Front. Microbiol.*, **9**, 47.
- Smith,J.D., Suresh,S., Schlecht,U., Wu,M., Wagih,O., Peltz,G., Davis,R.W., Steinmetz,L.M., Parts,L. and St Onge,R.P. (2016) Quantitative CRISPR interference screens in yeast identify chemical-genetic interactions and new rules for guide RNA design. *Genome Biol.*, **17**, 45.
- Chen,Y., Bao,J., Kim,I.K., Siewers,V. and Nielsen,J. (2014) Coupled incremental precursor and co-factor supply improves

- 3-hydroxypropionic acid production in *Saccharomyces cerevisiae*. *Metab. Eng.*, **22**, 104–109.
32. Qiu,C., Chen,X., Rexida,R., Shen,Y., Qi,Q., Bao,X. and Hou,J. (2020) Engineering transcription factor-based biosensors for repressive regulation through transcriptional deactivation design in *Saccharomyces cerevisiae*. *Microb. Cell Fact.*, **19**, 146.
 33. Liu,Z. and Myers,L.C. (2015) Fungal mediator tail subunits contain classical transcriptional activation domains. *Mol. Cell. Biol.*, **35**, 1363–1375.
 34. Chen,X., Azizkhan,J.C. and Lee,D.C. (1992) The binding of transcription factor Sp1 to multiple sites is required for maximal expression from the rat transforming growth factor alpha promoter. *Oncogene*, **7**, 1805–1815.
 35. Conlan,R.S., Gounalaki,N., Hatzis,P. and Tzamarias,D. (1999) The TUP1-cyc8 protein complex can shift from a transcriptional co-repressor to a transcriptional co-activator. *J. Biol. Chem.*, **274**, 205–210.
 36. Jabet,C., Sprague,E.R., VanDemark,A.P. and Wolberger,C. (2000) Characterization of the N-terminal domain of the yeast transcriptional repressor TUP1. Proposal for an association model of the repressor complex TUP1 x ssn6. *J. Biol. Chem.*, **275**, 9011–9018.
 37. Zetsche,B., Gootenberg,J.S., Abudayyeh,O.O., Slaymaker,I.M., Makarova,K.S., Essletzbichler,P., Völz,S.E., Joung,J., van der Oost,J., Regev,A. et al. (2015) Cpf1 is a single RNA-guided endonuclease of a class 2 CRISPR-Cas system. *Cell*, **163**, 759–771.
 38. Ciurkot,K., Gorochowski,T.E., Roubos,J.A. and Verwaal,R. (2021) Efficient multiplexed gene regulation in *Saccharomyces cerevisiae* using dCas12a. *Nucleic Acids Res.*, **49**, 7775–7790.
 39. Swiat,M.A., Dashko,S., den Ridder,M., Wijsman,M., van der Oost,J., Daran,J.M. and Daran-Lapujade,P. (2017) FnCpf1: a novel and efficient genome editing tool for *Saccharomyces cerevisiae*. *Nucleic Acids Res.*, **45**, 12585–12598.
 40. Nehlin,J.O. and Ronne,H. (1990) Yeast MIG1 repressor is related to the mammalian early growth response and Wilms' tumour finger proteins. *EMBO J.*, **9**, 2891–2898.
 41. Jers,C., Kalantari,A., Garg,A. and Mijakovic,I. (2019) Production of 3-Hydroxypropanoic acid from glycerol by metabolically engineered bacteria. *Front. Bioeng. Biotechnol.*, **7**, 124.
 42. Henry,C.S., Broadbelt,L.J. and Hatzimanikatis,V. (2010) Discovery and analysis of novel metabolic pathways for the biosynthesis of industrial chemicals: 3-hydroxypropanoate. *Biotechnol. Bioeng.*, **106**, 462–473.
 43. Shi,S., Chen,Y., Siewers,V. and Nielsen,J. (2014) Improving production of malonyl coenzyme A-derived metabolites by abolishing Snf1-dependent regulation of Acc1. *Mbio*, **5**, e01130-14.
 44. Schweizer,M., Roberts,L.M., Höltke,H.J., Takabayashi,K., Höllerer,E., Hoffmann,B., Müller,G., Köttig,H. and Schweizer,E. (1986) The pentafunctional FAS1 gene of yeast: its nucleotide sequence and order of the catalytic domains. *Mol. Gen. Genet.*, **203**, 479–486.
 45. Mohamed,A.H., Chirala,S.S., Mody,N.H., Huang,W.Y. and Wakil,S.J. (1988) Primary structure of the multifunctional alpha subunit protein of yeast fatty acid synthase derived from FAS2 gene sequence. *J. Biol. Chem.*, **263**, 12315–12325.
 46. Qiu,C., Huang,M., Hou,Y., Tao,H., Zhao,J., Shen,Y., Bao,X. and Qi,Q. (2022) Biosensor-Coupled in vivo mutagenesis and omics analysis reveals reduced lysine and arginine synthesis to improve malonyl-coenzyme A flux in *Saccharomyces cerevisiae*. *mSystems*, **7**, e0136621.
 47. Nielsen,J. and Keasling,J.D. (2016) Engineering cellular metabolism. *Cell*, **164**, 1185–1197.
 48. Marella,E.R., Holkenbrink,C., Siewers,V. and Borodina,I. (2018) Engineering microbial fatty acid metabolism for biofuels and biochemicals. *Curr. Opin. Biotechnol.*, **50**, 39–46.
 49. Nguyen,T.V. and Lister,R. (2021) Genomic targeting of TET activity for targeted demethylation using CRISPR/Cas9. *Methods Mol. Biol.*, **2272**, 181–194.
 50. Mo,J., Chen,Z., Qin,S., Li,S., Liu,C., Zhang,L., Ran,R., Kong,Y., Wang,F., Liu,S. et al. (2020) TRADES: targeted RNA demethylation by suntag system. *Adv. Sci. (Weinh.)*, **7**, 2001402.